Contribution from the Department of Chemistry, University of Queensland, St. Lucia, QLD 4072, Australia, Department of Analytical Chemistry, University of New South Wales, P.O. Box 1, Kensington, NSW 2033, Australia, Research School of Chemistry, Australian National University, G.P.O. Box 4, Canberra, ACT 2601, Australia, and Institut für Anorganische und Physikalische Chemie, Universität Bern, CH-3000 Bern 9, Freiestrasse 3, Switzerland

Optical Study of the Near-Infrared Emission and Absorption in the Strongly Exchange-Coupled Dimer $Cs_3Mo_2Cl_9$

Robert Stranger,*,† Grainne Moran,‡ Elmars Krausz,§ Lucjan Dubicki,§ Hans Güdel,∥ and Naomi Furer∥

Received September 24, 1991

Highly structured near-infrared emission has been observed from single-crystal $Cs_3Mo_2Cl_9$ for the first time, corresponding to the spin-allowed $^3E''(^3A_2{}^1E) \rightarrow {}^3A_2''(^3A_2{}^3A_2)$ pair transition. The spectroscopically determined singlet-triplet ground-state exchange splitting is approximately 842 cm^{-1}, in excellent agreement with 840 ± 50 cm^{-1} obtained from earlier ground-state magnetic studies. The emission spectrum is dominated by long progressions in the ν(Mo-Mo) stretching mode of 111 cm^{-1}, based on two static origins separated by 50 cm^{-1}. The ν(Mo-Mo) stretching mode is reduced some 31 cm^{-1} from that of the $^1A_1'(^3A_2{}^3A_2)$ ground state, indicating significant weakening of metal-metal bonding in the $^3A_2''(^3A_2{}^3A_2)$ excited state. Band shape analysis results in Huang-Rhys parameters of approximately 2.8 and 3.6 for the two progressions, corresponding to lengthening of the Mo-Mo bond by approximately 0.09 and 0.10 Å, respectively. The large zero-field splitting of 50 cm^{-1} observed for the $^3A_2''(^3A_2{}^3A_2)$ ground pair state is consistent with calculated values based on a perturbation treatment of the pair configuration in the Mo-Mo σ bond limit. A temperature-dependence study of thick single crystals of $Cs_3Mo_2Cl_9$ indicates that the entire 8000-cm^{-1} absorption band is due to the $^1A_1'(^3A_2{}^3A_2) \rightarrow {}^3E''(^3A_2{}^1E)$ pair transition only, and this is consistent with the moderate Mo-Mo π interaction observed previously for the double-excitation region between 12 500 and 15 500 cm^{-1}. From the spectroscopic analysis, the $A_1' + A_2'$, E'', and E' spin-orbit levels of the $^3E''(^3A_2{}^1E)$ multiplet were located with $A_1' + A_2'$ established as the emitting level. At low temperatures, evidence exists for a small departure from strict D_{3h} selection rules.

Introduction

The electronic structure of the exchange-coupled $Mo_2Cl_9^{3-}$ dimer has been investigated both experimentally and theoretically in a number of studies.[1-4] Initially, we presented an overall study of the absorption bands below 16 000 cm^{-1} in $Cs_3Mo_2Cl_9$ and assigned the transitions on the basis of an exchange-coupled pair model involving the full $t_2{}^3t_2{}^3$ pair configuration.[1] The observed bands were consistent with those predicted for an effective $t_{2e}{}^2t_{2e}{}^2$ pair configuration resulting from significant σ overlap of the trigonal t_{2z} metal orbitals. Although the Mo-Mo σ bonding was shown to be quite strong (J_σ = 20 000 ± 5000 cm^{-1}), it was not possible to obtain a reliable estimate of the Mo-Mo π interaction. In fact, conflicting results as to the magnitude of J_π were found for the singly- and doubly-excited pair states. On the basis of assignments made for the $^3E'$ and $^3E''$ multiplets belonging to the singly-excited $^3A_2{}^1E$ pair state at approximately 8000 cm^{-1}, it was concluded that the Mo-Mo π interaction was quite weak with J_π less than 500 cm^{-1}. However, a later study,[2] involving a temperature-dependence analysis of the $^1E{}^1E$ double-excitation region around 13 000 cm^{-1}, indicated that J_π was not small but approximately 7000 cm^{-1}, representing around 30% of the value of J_σ.

More recently,[3] the theoretical model was extended to include the cubic e_g orbitals, as the $t_2{}^3t_2{}^3$ pair model is only valid for small J_π. Using this model, it was possible to rationalize the anomalously low orbital g values found for both singly- and doubly-excited pair states in terms of extensive mixing of the single-ion t_{2e} and e_g orbitals by the Mo-Mo π interaction. This work confirmed the presence of a moderate Mo-Mo π interaction, $J_\pi \approx$ 7000 cm^{-1}, in both the singly- and doubly-excited pair states. For $J_\pi \approx$ 7000 cm^{-1}, the $^3E'$ multiplet is calculated to lie some 3000 cm^{-1} to higher energy[3] and most likely overlaps with the singly-excited $^3A_2{}^1A_1$ pair state observed near 11 500 cm^{-1}. Consequently, it is necessary to reexamine the singly-excited $^3A_2{}^1E$ pair state absorption near 8000 cm^{-1} in order to see if the fine structure originates from only one $^3A_2{}^1E$ multiplet, namely $^3E''$. Furthermore, the $A_1' + A_2'$ and E'' spin-orbit levels of the $^3E''$ multiplet have yet to be located.

Calculations based on the extended theoretical model[3] predict a ground-state exchange splitting nearly twice as large as that obtained from temperature-dependent magnetic susceptibility measurements.[4,5] Since luminescence spectroscopy has enabled accurate exchange splittings to be determined for a range of Cr(III) dimers,[6-8] it is possible that $Mo_2Cl_9^{3-}$ will also undergo emission. The lowest energy excited-state absorption occurs around 8000 cm^{-1}, corresponding to the singly-excited $^3A_2{}^1E$ pair state. Accordingly, we have used a highly sensitive Ge detector to probe for near-infrared luminescence in order to investigate, spectroscopically, the ground-state exchange splitting.

Experimental Section

Crystals of $Cs_3Mo_2Cl_9$ were obtained by two different methods and in different laboratories. Small crystals were grown by sublimation from a fused stoichiometric mixture of CsCl and $MoCl_3$.[1] Alternatively, crystals were grown from powdered $Cs_3Mo_2Cl_9$ by the Bridgeman method, the Mo-Mo axis of the dimer being perpendicular to the direction of growth.

The apparatus used for absorption and luminescence measurements has recently been described.[9] In relation to earlier work, a recalibration of the original grating has shown that the previously reported band positions[1] between 7700 and 8200 cm^{-1} are incorrect and should be shifted by 18 Å (≈11 cm^{-1}) to lower energy. The corrected band positions are given in this work.

For steady-state luminescence spectra, a high sensitivity, liquid N_2 cooled Ge detector (Applied Detector Corp.) was used. The 488-nm line of an Ar^+ ion laser was used for excitation, and the luminescence was dispersed with a Spex 1401 monochromator fitted with a 1.6-μm blaze grating. For excitation and lifetime measurements, a PAR N_2-pumped dye laser provided excitation wavelengths from 645 to 675 nm using the dye DCM (Exciton). The total emission was detected using a series of cutoff filters and a liquid N_2 cooled InSb detector having a response time better than 5 ns. Lifetimes were measured using a Tektronix 2430 digital oscilloscope.

Results and Discussion

Absorption Spectrum. The 1.6 K orthoaxial absorption spectra

† University of Queensland.
‡ University of New South Wales.
§ Australian National University.
∥ Universität Bern.

(1) Dubicki, L.; Krausz, E.; Stranger, R.; Smith, P. W.; Tanabe, Y. *Inorg. Chem.* **1987**, *26*, 2247.
(2) Stranger, R. *Chem. Phys. Lett.* **1989**, *157*, 472.
(3) Stranger, R. *Inorg. Chem.* **1990**, *29*, 5231.
(4) Grey, I. E.; Smith, P. W. *Aust. J. Chem.* **1971**, *24*, 73.
(5) Stranger, R.; Smith, P. W.; Grey, I. E. *Inorg. Chem.* **1989**, *28*, 1271.
(6) Riesen, H.; Güdel, H. U. *Mol. Phys.* **1986**, *58*, 509.
(7) Riesen, H.; Güdel, H. U. *Mol. Phys.* **1987**, *60*, 1221.
(8) Riesen, H.; Reber, C.; Güdel, H. U.; Wieghardt, K. *Inorg. Chem.* **1987**, *26*, 2747.
(9) Stranger, R.; Moran, G.; Krausz, E.; Güdel, H.; Furer, N. *Mol. Phys.* **1990**, *69*, 11.
(10) Lever, A. B. P. *Inorganic Electronic Spectroscopy*; Elsevier: Amsterdam, **1984**.
(11) Smith, P. W.; Stranger, R. *Aust. J. Chem.* **1986**, *39*, 1269.
(12) Wilson, R. B.; Solomon, E. I. *J. Am. Chem. Soc.* **1980**, *102*, 4085.

0020-1669/92/1331-2860$03.00/0

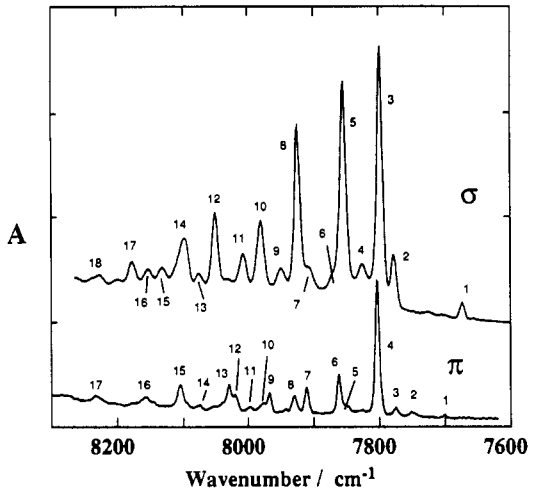

Figure 1. Polarized absorption spectra of $Cs_3Mo_2Cl_9$ at 1.5 K.

of the $^3A_2{}^3A_2 \rightarrow {}^3A_2{}^1E$ pair-state transition in $Cs_3Mo_2Cl_9$ between 7600 and 8300 cm^{-1} is shown in Figure 1. The spectra are identical to those previously reported[1] except a thicker crystal has been used to resolve weaker features and identify hot bands. The σ spectrum consists principally of progressions in the totally symmetric mode, $\nu_4 = 127$ cm^{-1}, built on two origins at 7797 and 7854 cm^{-1}. The π spectrum has only one major origin, located at 7802 cm^{-1}, from which a weak progression in the $\nu_4 = 127$ cm^{-1} totally symmetric mode occurs.

In the absence of any Mo–Mo π interaction ($J_\pi = 0$), the $^3E''$ and $^3E'$ muliplets belonging to the $^3A_2{}^1E$ singly-excited pair state are degenerate, but for non-zero J_π they split with $^3E'$ lying at higher energy (see Figure 2 of ref 3). The $^3E''$ and $^3E'$ multiplets comprise $A_1' + A_2' + E' + E''$ and $A_1'' + A_2'' + E' + E''$ spin–orbit levels, respectively, with electric dipole transitions allowed from the $^1A_1'(^3A_2{}^3A_2)$ ground state to $A_2''(\pi)$ and $E'(\sigma)$ spinor states. From an earlier mangetooptical study,[1] the σ origin at 7797 cm^{-1} was firmly established as the $^3E''(E')$ spin–orbit level. The 7854-cm^{-1} σ origin could not be attributed to the $^3E'(E')$ spin–orbit level, as this assignment was not consistent with the sign of the observed g value. Instead, it was assigned as a vibronic involving one quantum of an E vibration, but it was not possible to distinguish between $^3E'(E') \times \nu(E')$ or $^3E''(E'') \times \nu(E'')$. The transverse Zeeman spectrum ($H \| z$) of the main π origin at 7802 cm^{-1} was consistent with an $A_1'' + A_2''$ spin–orbit doublet having a zero-field splitting of $\approx$5 cm^{-1}, with A_1'' lying at higher energy. An obvious assignment was the $^3E'(A_1'' + A_2'')$ spin–orbit level, but the possibility of the vibronic origin $^3E''(A_1' + A_2') \times \nu(A_2'')$ or $^3E''(A_1' + A_2') \times \nu(A_1'')$ was not dismissed.

From the earlier assignment of the 7797 (σ) and 7802 (π) cm^{-1} origins to $^3E''(E')$ and $^3E'(A_1'' + A_2'')$ spin–orbit levels, respectively, the Mo–Mo π interaction was assumed to be quite small with $J_\pi < 500$ cm^{-1}, but this conflicted with the much larger interaction of $J_\pi \approx 7000$ cm^{-1} found for the doubly-excited pair-state transitions between 12 700 and 15 500 cm^{-1}.[2] Since earlier evidence for the close proximity of the $^3E'$ and $^3E''$ multiplets relied on the assignment of the π origin at 7802 cm^{-1} to $^3E'(A_1'' + A_2'')$, the temperature dependence of the π spectrum was examined in order to locate possible vibronic origins.

1. π Polarization. The π spectrum from 7500 to 7900 cm^{-1} at 1.5, 20, 50, and 75 K is shown in Figure 2a. Above 50 K, a hot band appears at 7600 cm^{-1}. Under the assumption that this band is associated with the 7802-cm^{-1} cold line, the true origin is placed at $\approx$7701 cm^{-1} with an inducing mode frequency of 101 cm^{-1}. It is unlikely that the 7600-cm^{-1} hot band is associated with another π origin, as they occur 60 cm^{-1} or more to higher energy and, being much weaker, are unlikely to lead to the appearance of hot bands at 50 K. The vibronic nature of the 7802-cm^{-1} π line eliminates the previous assignment as $^3E'(A_1'' + A_2'')$ and, therefore, must be assigned to $^3E''(A_1' + A_2')$. This spin–orbit level can acquire electric dipole intensity through coupling with either A_1'' or A_2'' vibrations. Since no A_2'' mode occurs around

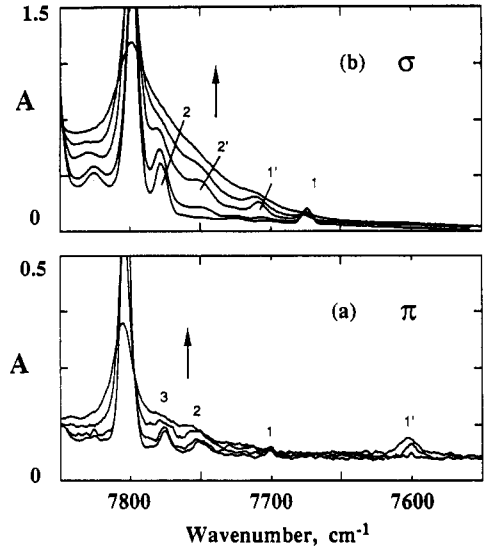

Figure 2. Temperature dependence of the σ and π absorption spectra in the 7800–7600-cm^{-1} origin region. Temperatures: (π) 1.5, 20, 50, 75 K; (σ) 10, 25, 50, 83, 112 K. Arrows indicate the sequence of spectra with an increase in temperature.

101 cm^{-1},[2] the inducing vibration is assigned as A_1'' which is both infrared and Raman inactive.

Further evidence for the $^3E''(A_1' + A_2')$ electronic origin at 7701 cm^{-1} comes from the appearance of a weak band at this position in the 1.5 K π spectrum (see Figure 2a). For strict D_{3h} symmetry appropriate to the $Mo_2Cl_9^{3-}$ anion, the transition from $^1A_1'(^3A_2{}^3A_2)$ to the $^3E''(A_1' + A_2')$ spin–orbit level is both electric dipole and magnetic dipole forbidden in π polarization. However, a small axial crystal strain which removes the σ_h reflection plane will result in C_{3v} microsymmetry, making the $A_1' \rightarrow A_1'$ transition partially electric dipole allowed. In fact, evidence of this strain is seen elsewhere in the absorption spectrum of $Cs_3Mo_2Cl_9$.[13] The same phenomenon was also observed in the pair spectrum of the $(\mu\text{-}OH)_3Cr_2(Me\text{-}tacn)_2$ dimer.[7]

The π line at 7862 cm^{-1} has a transverse Zeeman splitting similar to the 7802-cm^{-1} line. Their separation of 60 cm^{-1} does not correspond to any totally symmetric mode. However, the separation of 161 cm^{-1} from the $A_1' + A_2'$ electronic origin at 7701 cm^{-1} corresponds closely to $\nu_3(A_2'')$.[2] Hence, the 7862-cm^{-1} π line is assigned to $^3E''(A_1' + A_2') \times \nu_3(A_2'')$. Other π lines at 7750, 7776, and 8029 cm^{-1} are assigned to $^3E''(A_1' + A_2')$ coupled with ν_5, ν_4, and ν_1 A_2'' modes, respectively.

On the basis of a large Zeeman splitting, the π lines at 7967, 8020, and 8105 cm^{-1} were assigned to the $^3E''(E')$ origin coupled with ν_3, ν_2, and ν_1 E'' vibrational modes, respectively.[1] Apart from the line at 7910 cm^{-1}, which is assigned to $^3E''(A_2') \times \nu(A_1'')$, the remaining π lines can be attributed to either progressions in the 127-cm^{-1} totally symmetric mode $\nu_4(A_1')$ or vibronics based on the $^3E''(E'')$ origin coupled with E' vibrations. The assignment of all observed π lines is detailed in Table I.

2. σ Polarization. The temperature dependence of the σ spectrum from 7500 to 7900 cm^{-1} is shown in Figure 2b. Two hot bands appear at 7708 and 7747 cm^{-1}. The former is associated with the cold line at 7854 cm^{-1} whereas the cold line associated with the latter hot band is obscured by the intense $^3E''(E')$ origin. This places the forbidden electronic origin at around 7779 cm^{-1}, with inducing modes of approximately 75 and 30 cm^{-1}. The 30-cm^{-1} mode corresponds to $\nu_6(E'')$. The 75-cm^{-1} mode could be either $\nu_5(E'')$ or $\nu_6(E')$, but in order to be consistent with the negative g_z value observed for the vibronic at 7854 cm^{-1}, coupling must occur with an E'' vibration.[1] Accordingly, the 75-cm^{-1} mode is assigned to $\nu_5(E'')$. The forbidden electronic origin at approximately 7779 cm^{-1} must therefore have E'' symmetry and is assigned to the $^3E''(E'')$ spinor state. Higher energy σ lines at

(13) Stranger, R. Unpublished work.
(14) Dubicki, L.; Tanabe, Y. *Mol. Phys.* **1977**, *34*, 1531.

Table I. Position and Assignment of σ and π Absorption Lines for the $^1A_1'(^3A_2{}^3A_2) \rightarrow {}^3E''(^3A_2{}^1E)$ Pair Transition in $Cs_3Mo_2Cl_9$

line[a]	position, cm^{-1}	polarization	assignment[b]
1′	7600	π	$A_2' - \nu(A_1'')$
1	7673	σ	impurity, $^1A_1' \rightarrow {}^5A_1'(E')$?
1	7701	π	$A_1' + A_2'$ origin
1′	7708	σ	$E'' - \nu_5(E'')$
2′	7747	σ	$E'' - \nu_6(E'')$
2	7750	π	$A_1' + \nu_5(A_2'')$
3	7776	π	E'' origin, $A_1' + \nu_4(A_2'')$
2	7777	σ	$(A_1' + A_2') + \nu_6(E')$
3	7797	σ	E' origin
4	7802	π	$A_2' + \nu(A_1'')$
4	7828	σ	$E'' + \nu_5(A_2'')$
5	7851	π	$E'' + \nu_6(E')$
5	7854	σ	$E'' + \nu_5(E'')$
6	7862	π	$A_1' + \nu_3(A_2'')$
6	7867	σ	$E' + \nu_6(E')$
7	7906	σ	$A_1' + \nu_5(A_2'') + \nu_4(A_1')^c$
7	7910	π	$(A_1' + A_2') + \nu_6(E') + \nu_4(A_1')^c$
8	7924	σ	$E' + \nu_4(A_1')^c$
8	7929	π	$A_2' + \nu(A_1'') + \nu_4(A_1')^c$
9	7950	σ	$E'' + \nu_3(E''/A_2'')$, $E' + \nu_4(E')$
9	7967	π	$E' + \nu_3(E'')$
10	7977	π	$A_2' + \nu(A_1'') + \nu_4(A'_1)^c + \nu_5(A_1')$
10	7981	σ	$E'' + \nu_5(E'') + \nu_4(A_1')^c$
11	7998	π	$A_1' + \nu_3(A_2'') + \nu_4(A_1')^c$
11	8007	σ	$E'' + \nu_5(E'') + \nu_4(E')$
12	8020	π	$E' + \nu_2(E'')$
13	8029	π	$A_1' + \nu_1(A_2'')$
12	8052	σ	$E' + 2\nu_4(A_1')^c$
14	8076	π	$A_1' + \nu_1(A_2'') + \nu_5(A_1')$
13	8078	σ	$E'' + \nu_3(E''/A_2'') + \nu_4(A_1')$,[c] $E' + \nu_4(A_1') + \nu_4(E')$
14	8096	σ	$E'' + \nu_1(A_2'')$
15	8105	π	$E' + \nu_1(E'')$
15	8133	σ	$E'' + \nu_5(E'') + \nu_4(A_1')^c + \nu_4(E')$
16	8153	σ	$E' + \nu_1(A_1')$
16	8158	π	$A_1' + \nu_1(A_2'') + \nu_4(A_1')^c$
17	8179	σ	$E' + 3\nu_4(A_1')^c$
18	8224	σ	$E'' + \nu_1(A_2'') + \nu_4(A_1')^c$
17	8233	π	$E' + \nu_1(E'') + \nu_4(A_1')^c$

[a] Single primes indicate hotbands. [b] Refer to Table II of ref 2 for vibrational assignments. [c] $\nu_4(A_1') = 127\ cm^{-1}$.

7828, 7950, 8007, and 8096 cm^{-1} can be attributed to coupling of the E″ origin with $\nu_5(A_2'')$, $\nu_3(E''/A_2'')$, $\nu_2(E'')$, and $\nu_1(E'')$ vibrations, respectively, while the lower energy σ origin at 7777 cm^{-1} is assigned to $^3E''(A_1' + A_2') \times \nu_6(E')$. It is also possible that the 7777-cm^{-1} line has a small contribution from the E″ origin due to a slight deviation from strict D_{3h} selection rules resulting from crystal strain. In general, all remaining σ lines can be assigned as progressions in the 127-cm^{-1} totally symmetric mode off the above origins. There is also some evidence for weak coupling off both the 7797- and 7854-cm^{-1} σ origins to the $\nu_4(E')$ Jahn-Teller-active mode at approximately 153 cm^{-1}.

A weak band occurs to lowest energy at 7673 cm^{-1} but does not appear to be related to any other lines associated with the $^3A_2{}^3A_2 \rightarrow {}^3A_2{}^1E$ pair-state transitions to higher energy. This line is therefore attributed to an impurity, although it is seen in all samples which were studied. There is the possibility that it corresponds to the σ polarized $^1A_1'(A_1') \rightarrow {}^5A_1'(E')$ pair-state transition within the exchange split $^3A_2{}^3A_2$ ground-state manifold, as calculations predict the $^5A_1'$ multiplet to lie approximately 6000–7000 cm^{-1} above the $^1A_1'$ ground state.[3] Although $\Delta S = 2$ transitions are forbidden, they may acquire intensity from higher order spin–orbit coupling processes. In this case, the intensity would derive from the nearby $^3E''(^3A_2{}^1E)$ multiplet. Assignments for all σ lines are detailed in Table I, while the observed splitting of the $^3E''(^3A_2{}^1E)$ multiplet is shown in Figure 3.

The above analysis has shown that the 8000-cm^{-1} absorption band in $Cs_3Mo_2Cl_9$ results from transitions from the $^1A_1'(^3A_2{}^3A_2)$ ground state to the $^3E''$ multiplet only of the singly-excited $^3A_2{}^1E$ pair state. The $A_1' + A_2'$, E″, and E′ spin–orbit levels of the $^3E''$ multiplet are located at 7701, 7776, and 7797 cm^{-1}, respectively.

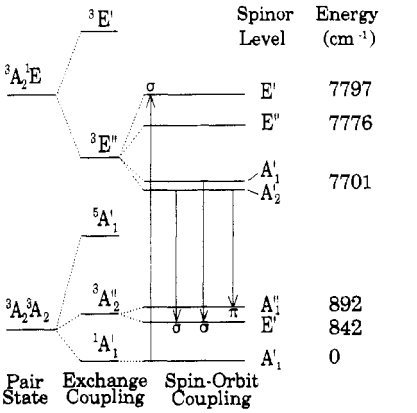

Figure 3. Energy diagram for the ground $^3A_2{}^3A_2$ and singly-excited $^3A_2{}^1E$ pair states for $Cs_3Mo_2Cl_9$, showing the splitting resulting from exchange-coupling and spin–orbit coupling interactions. The pair multiplets and spin–orbit levels are labeled on the basis of D_{3h} symmetry.

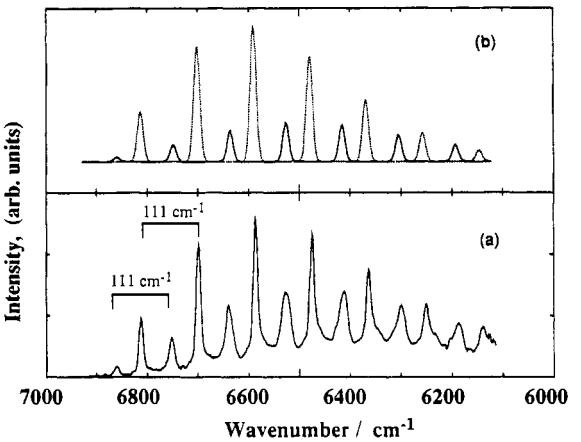

Figure 4. (a) Unpolarized luminescence spectrum (corrected) of $Cs_3Mo_2Cl_9$ at 1.6 K. (b) Simulated spectrum based on a progression of 111 cm^{-1} off two origins at 6859 cm^{-1} (—) and 6809 cm^{-1} (···) with Huang Rhys factors of 4.0 and 2.5, respectively.

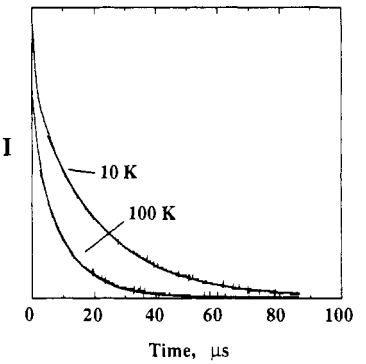

Figure 5. Luminescence decay curves at 10 and 100 K. Decays are close to single exponential. Calculated curves are fitted to data in the range 4–85 μs.

Luminescence Spectrum. The unpolarized luminescence spectrum of $Cs_3Mo_2Cl_9$ is shown in Figure 4a. The origin of luminescence is at 6859 cm^{-1}, some 940 cm^{-1} lower in energy than the lowest observed features in absorption. No luminescence could be detected at higher energy, and no absorption was observed in the 6000–7000-cm^{-1} region, even in crystals 0.5 cm thick. The lifetime of luminescence was found to be 21.4 μs at 10 K and 10.3 μs at 100 K, with decay curves being approximately single exponential in both cases (see Figure 5). A similar luminescence spectrum, shifted to about 5 cm^{-1} higher energy, was also observed for $K_3Mo_2Cl_9$. No luminescence could be detected for $Cs_3Mo_2Br_9$ in either the visible or near-infrared regions. Polarization of

luminescence experiments were attempted on $Cs_3Mo_2Cl_9$, but the data obtained were not reliable enough to be used in the analysis.

Since the emission for neat $Cs_3Mo_2Cl_9$ is relatively weak, the possibility arises that it may be due to an impurity populated by efficient energy transfer from $Mo_2Cl_9^{3-}$, though crystals grown by different methods and in different laboratories gave similar results. Monomeric Mo(III) chloro species would be expected to emit at energies higher or lower than that observed, corresponding to the $^2E \rightarrow {}^4A_2$ and $^2T_2 \rightarrow {}^2E, {}^2T_1$ transitions.[9] While there are a range of chloromolybdenum dimers reported,[10] none were found having transitions in the 6600–7000-cm^{-1} range.

To check the origin of emission, an excitation spectrum was measured between 645 and 675 nm, corresponding to a strong π polarized band in absorption.[1] The excitation spectrum showed the same structure as the absorption band, though because of strong absorption of even a thin crystal in this range, the relative intensities of the peaks were not reproduced. Apart from broadening of the fine structure, the luminescence intensity is not very temperature sensitive up to 70 K. In contrast, energy transfer to an impurity would be expected to become more efficient with increasing temperature. The emission is therefore assigned as intrinsic to the $Mo_2Cl_9^{3-}$ dimer and, since the origin is nearly 1000 cm^{-1} lower in energy than the first observed transition in absorption, is assigned to the $^3E''(^3A_2{}^1E) \rightarrow {}^3A_2''(^3A_2{}^3A_2)$ spin-allowed pair-state transition. This parallels studies of weakly coupled Cr^{3+} dimers where the most intense luminescence was observed from the lowest energy-excited spin-triplet state to the triplet spin level of the exchange split ground state.[6-8]

The luminescence spectrum shown in Figure 4a consists of two long progressions built on two origins at 6859 and 6809 cm^{-1}. Both progressions are based on a mode of approximately 111 cm^{-1}, which does not correspond to any ground-state frequency of $Cs_3Mo_2Cl_9$.[2,11] However, a reduction of approximately 15 cm^{-1} in the ground-state totally symmetric Mo–Mo stretching mode of 142 cm^{-1} occurs in absorption for the singly-excited $^3A_2{}^3A_2 \rightarrow {}^3A_2{}^1E$ pair-state transition, as ν(Mo–Mo) was observed at 127 cm^{-1}.[1] This reduction is approximately 30 cm^{-1} in the emission spectrum and implies weaker Mo–Mo bonding in the $^3A_2''(^3A_2{}^3A_2)$ ground-state level relative to the singly-excited and doubly-excited pair states as well as the $^1A_1'(^3A_2{}^3A_2)$ ground state. The large reduction in ν(Mo–Mo) in the triplet $^3A_2''$ ground-state level, compared to the singlet $^1A_1'$ ground-state level, can be attributed to the σ antibonding character mixed into the former due to configuration interaction with the $^3A_2''(\sigma \rightarrow \sigma^*)$ excited state. The differences in the equilibrium geometries may account for the discrepancy between the observed ($\approx$880 cm^{-1}) and calculated ($\approx$1500 cm^{-1}) ground-state exchange splittings, as the latter was determined on the basis of exchange parameters derived from excited-pair-state assignments.

Within the harmonic approximation, assuming the vibrational frequency is the same in the ground and excited states, the band shape resulting from a single mode progression can be generated using the expression[12]

$$I(E) = \sum_{n=0} \exp(-S)\frac{S^n}{n!} g_o(E - nh\nu)$$

where g_o is a line shape function (assumed to be gaussian) describing the origin, n is the vibrational quantum number in a progressional mode Q, and S is the Huang-Rhys parameter given by

$$S = \frac{1}{2}k(\Delta Q)^2/h\nu$$

with force constant k and displacement ΔQ. Since the observed luminescence comprises progressions in a single mode off two origins, the overall intensity distribution will be a sum of two band shape expressions, $I(E) = I_1(E) + I_2(E)$, with different Huang-Rhys parameters S_1 and S_2. As shown in Figure 4b, the best fit to the observed band shape (based on peak heights) occurs for $S_1 = 2.5$ and $S_2 = 4.0$ for the strong and weak progressions, respectively. A fit based on relative peak intensities gives $S_1 = 2.8$ and $S_2 = 3.6$. The fits are only approximate, particularly for the weaker progression, as the observed emission suffers from a significant baseline problem. Futhermore, as discussed below, the weaker progression represents the superposition of two progressions due to the $\sim$5-cm^{-1} zero-field splitting of the $A_1' + A_2'$ emitting level.

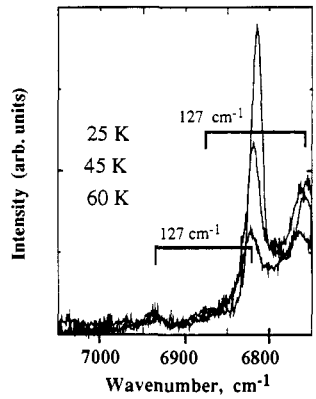

Figure 6. Temperature dependence of the luminescence spectrum in the origin region at 25, 45, and 60 K. The 25 K spectrum is the most intense.

The Huang-Rhys parameter S is related to the displacement ΔQ (in Å) along the vibrational coordinate Q through[15]

$$\Delta Q = 8.21\left(\frac{S}{\mu}\right)^{1/2}\left(\frac{\nu_i + \nu_f}{2\nu_i\nu_f}\right)^{1/2}$$

where μ is the reduced mass (amu) and ν_i and ν_f are the initial and final state vibration frequencies, 127 and 111 cm^{-1}, respectively. The reduced mass will lie between the diatomic $(Cl_3Mo)(MoCl_3)$ and triatomic $(Cl_3Mo)(Cl_3)(MoCl_3)$ limits. In the triatomic limit the reduced mass is approximated by $\mu = M(MoCl_3)$, and the Huang-Rhys parameters of $S_1 = 2.8$ and $S_2 = 3.6$ result in Mo–Mo displacements of $\Delta Q_1 = 0.09$ Å and $\Delta Q_2 = 0.10$ Å, respectively. The calculated Mo–Mo displacements must be considered as maximum possible values, as a normal coordinate analysis of $Mo_2Cl_9^{3-}$ has shown that considerable mode mixing occurs, with the A_1' breathing mode containing less than 10% Mo–Mo stretching character.[16] Interestingly, in the case of tetrakis(μ-trifluoroacetato)dimolybdenum(III),[17,18] it has been shown that the assumption of only one normal mode involved in the excited-state distortion led to an exagerated Mo–Mo displacement by a factor of approximately 2.[18]

In order to ascertain whether the origins at 6859 and 6809 cm^{-1} are static or vibronically induced, the temperature dependence of luminescence was measured up to 60 K, as shown in Figure 6. At 60 K, two hot bands are apparent at higher energy at 6936 and 6875 cm^{-1}, though the latter is very weak. Both hot bands are located 127 cm^{-1} to higher energy from the cold bands at 6809 and 6748 cm^{-1}. The 127-cm^{-1} separation corresponds exactly to the totally symmetric frequency $\nu_4(A_1')$ observed in the absorption spectrum between 7800 and 8200 cm^{-1}. The hot bands are therefore attributed to population of the $v = 1$ vibrational level of the excited emitting state. The absence of vibronic hot bands indicates that the emission lines at 6859 and 6809 cm^{-1} are either static in origin or induced by high-frequency vibrations.

The emission is assumed to originate from the $A_1' + A_2'$ spin–orbit state, as this has been established as the lowest energy $^3E''$ spin–orbit level from the above absorption study. The same transition dominated the emission found in the recent study of the $(\mu\text{-}OH)_3Cr_2(Me\text{-}tacn)_3$ dimer, with similar lifetimes also observed.[7] Neglecting the gound-state $^3A_2''$ zero-field splitting, the spectroscopically determined ground-state exchange splitting is therefore approximately 842 cm^{-1}, in excellent agreement with

(15) Miskowski, V. M.; Brinza, D. E. *J. Am. Chem. Soc.* **1986**, *108*, 8296.
(16) Stranger, R. Ph.D. Thesis, University of Tasmania, 1987.
(17) Trogler, W. C.; Solomon, E. I.; Trajberg, I.; Ballhausen, C. J.; Gray, H. B. *Inorg. Chem.* **1977**, *16*, 828.
(18) Zink, J. I. *Coord. Chem. Rev.* **1985**, *64*, 93.
(19) Trogler, W. C. *Inorg. Chem.* **1980**, *19*, 697.

the value of 840 ± 50 cm^{-1} found from the temperature dependence of magnetic susceptibility measurements.[4,5]

From Figure 3, three transitions from the $^3E''(A_1' + A_2')$ spin–orbit level to the $^3A_2''(A_1'' + E')$ ground-state spin–orbit levels are electric dipole allowed, corresponding to $A_1' \rightarrow E'(\sigma)$, $A_2' \rightarrow E'(\sigma)$, and $A_2' \rightarrow A_1''(\pi)$. The two σ polarized transitions will occur close together, as the A_1' and A_2' spin–orbit states belonging to the $^3E''$ multiplet are only separated by ≈5 cm^{-1}. The emission origins at 6859 and 6809 cm^{-1} are therefore attributed to $^3E''(A_1' + A_2') \rightarrow {}^3A_2''(E')$ and $^3E''(A_2') \rightarrow {}^3A_2''(A_1'')$, but without polarization data it is difficult to discriminate further. However, the vibrational bands associated with the weaker progression based on the 6859-cm^{-1} origin are distinctively broader and asymmetric, indicative of the $^3E''(A_1' + A_2') \rightarrow {}^3A_2''(E')$ transition due to the zero-field splitting of the A_1' and A_2' spinor levels.

From the above assignments, the zero-field splitting of the $^3A_2''(A_1'' + E')$ ground state is quite large, ≈50 cm^{-1}, with the E' level at lower energy. Although at this stage it is not possible to undertake a full d^3d^3 pair calculation which includes the spin–orbit interaction, due to the large basis size of 14 400, some measure of the zero-field splitting of the $^3A_2''(^3A_2{}^3A_2)$ pair state can be gained from the following perturbation treatment.

In the Mo–Mo σ bond limit, the $^3A_2''$ pair state derives from the t_{2e}^2 single-ion $^3A_2$ state for which the zero-field splitting is described by the spin-Hamiltonian

$$\mathcal{H}_{eff} = D[S_z^2 - S(S+1)/3]$$

with eigenvalues $|M = 0\rangle = -2D/3$ and $|M = \pm 1\rangle = D/3$. Second-order spin–orbit coupling must be invoked in order to split the $|M = 0\rangle$ and $|M = \pm 1\rangle$ spin levels of the $^3A_2$ state. Of the t_{2e}^2 excited states ^1E and $^1A_1$, only the $^1A_1$ level is coupled to the $^3A_2$ ground state according to

$$\langle {}^3A_2\ M = 0|\zeta \sum_i l_z s_z|{}^1A_1\rangle = i\zeta$$

where ζ is the one-electron spin–orbit coupling constant. For second-order perturbation, the energy shift of the $|M = 0\rangle$ level is given by

$$\langle {}^3A_2|\mathcal{H}_{so}|{}^1A_1\rangle\langle {}^1A_1|\mathcal{H}_{so}|{}^3A_2\rangle / E({}^3A_2 - {}^1A_1)$$

resulting in the zero-field splitting

$$D = E(|M = \pm 1\rangle - |M = 0\rangle) = \zeta^2/\Delta E$$

where $\Delta E = 12B + 4C$ is the energy difference between the $^1A_1$ and $^3A_2$ states and B and C are the usual Racah electron repulsion parameters.[3] For the single-ion $^3A_2$ state the $|M = 0\rangle$ level is predicted to lie at lower energy, whereas for the $^3A_2''(^3A_2{}^3A_2)$ pair state it can be shown that the splitting is reversed with the $|M = \pm 1\rangle$ level at lower energy. For Mo(III), the free ion spin–orbit coupling constant ζ is approximately 800 cm^{-1}, while from the low-temperature absorption spectrum of $Cs_3Mo_2Cl_9$, the separation of the single-ion $^1A_1$ and $^3A_2$ states is about 11 000 cm^{-1}. From these values, a zero-field splitting of $D \approx 60$ cm^{-1} is calculated for the $^3A_2''$ pair state with the $E'(M \pm 1)$ spin–orbit level at lower energy, in agreement with the above analysis. Allowing for an appropriate reduction in ζ from the free ion value ($\zeta \approx 600$ cm^{-1} was found from a spectroscopic study[9] of $MoCl_6^{3-}$), the observed zero-field splitting of ≈50 cm^{-1} seems quite reasonable.

Registry No. $Cs_3Mo_2Cl_9$, 29013-02-3; Mo, 7439-98-7.

Contribution from the Institut de Chimie Minérale et Analytique, Université de Lausanne, Place du Château 3, Lausanne CH-1005, Switzerland, and Department of Chemistry, University of the Orange Free State, Bloemfontein 9300, South Africa

^{13}C and ^{17}O NMR Studies of the Solution and Equilibrium Behavior of Selected Oxocyanorhenate(V) Complexes

Andreas Roodt,*[,1] Johann G. Leipoldt,[1] Lothar Helm,[2] and André E. Merbach*[,2]

Received January 23, 1992

Carbon-13 and oxygen-17 NMR spectroscopies were utilized to study the solution and protonation equilibrium behavior of the *trans*-dioxotetracyanorhenate(V) ion. The pK_{a_1} and pK_{a_2} values for the successive dissociation of the $[ReO(H_2O)(CN)_4]^-$ complex were determined from ^{13}C and ^{17}O NMR chemical shifts as 1.31 (7) and 3.72 (5), respectively. The dimeric species $[Re_2O_3(CN)_8]^{4-}$ (formed by condensation of $[ReO(OH)(CN)_4]^{2-}$ ions) and the monosubstituted product $[ReO(NCS)(CN)_4]^{2-}$ were also studied, and results were correlated with NMR measurements in DMSO solutions. The ^{17}O chemical shifts for the different species studied showed a direct relationship with X-ray crystal structure and infrared data and with the electron density on the coordinated oxygen ligands and demonstrated the effectiveness of ^{17}O NMR spectroscopy for characterization of these types of complexes.

Introduction

There have been differences in opinion in the literature on the nature of the different Re(V) species formed in solution when the *trans*-$[ReO_2(CN)_4]^{3-}$ complex is dissolved in acidic solution.[3,4] We have however eliminated the uncertainties by several X-ray crystal structure determinations[5] and kinetic[6] and infrared[7] studies over the last few years and showed that the aqueous acid chemistry of the $[ReO_2(CN)_4]^{3-}$ complex may be described by the reactions in Scheme I. Similar behavior has been confirmed previously for the isoelectronic Mo(IV)[8] and W(IV)[9] systems and recently

Scheme I

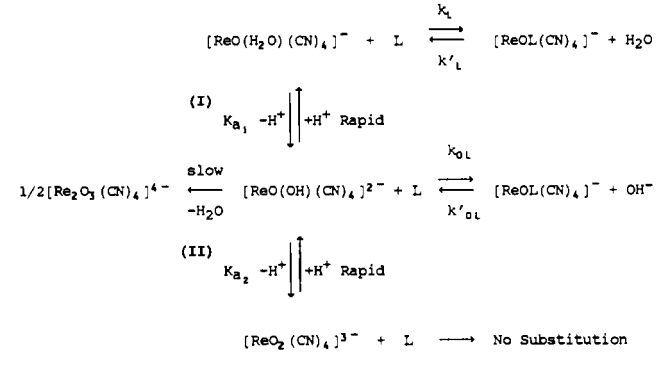

(1) University of the Orange Free State.
(2) Université de Lausanne.
(3) Chakravorti, M. C. *J. Inorg. Nucl. Chem.* **1972**, *34*, 893.
(4) Toppen, D.; Murmann, R. K. *Inorg. Chem.* **1973**, *12*, 1611.
(5) (a) Purcell, W.; Roodt, A.; Basson, S. S.; Leipoldt, J. G. *Transition Met. Chem. (London)* **1989**, *14*, 369. (b) Basson, S. S.; Leipoldt, J. G.; Roodt, A.; Purcell, W. *Transition Met. Chem. (London)* **1987**, *12*, 82. (c) Purcell, W.; Roodt, A.; Basson, S. S.; Leipoldt, J. G. *Transition Met. Chem. (London)* **1989**, *14*, 5. (d) Purcell, W.; Roodt, A.; Basson, S. S.; Leipoldt, J. G. *Transition Met. Chem. (London)* **1990**, *15*, 239.
(6) (a) Purcell, W.; Roodt, A.; Basson, S. S.; Leipoldt, J. G. *Transition Met. Chem. (London)* **1989**, *14*, 224. (b) Purcell, W.; Roodt, A.; Leipoldt, J. G. *Transition Met. Chem. (London)* **1991**, *17*, 339.
(7) Leipoldt, J. G.; Basson, S. S.; Roodt, A.; Purcell, W. *Transition Met. Chem. (London)* **1987**, *12*, 209.

0020-1669/92/1331-2864$03.00/0